Available online at www.sciencedirect.com
SCIENCE DIRECT®
Proceedings of the Combustion Institute 30 (2005) 1283–1292
Proceedings of the Combustion Institute
www.elsevier.com/locate/proci

An optimized kinetic model of H_2/CO combustion

Scott G. Davis[a,*], Ameya V. Joshi[a], Hai Wang[a], Fokion Egolfopoulos[b]

[a] Department of Mechanical Engineering, University of Delaware, Newark, DE 19716, USA
[b] Department of Aerospace and Mechanical Engineering, University of Southern California, Los Angeles, CA 90089, USA

Abstract

We propose a H_2–CO kinetic model which incorporates the recent thermodynamic, kinetic, and species transport updates relevant to high-temperature H_2 and CO oxidation. Attention has been placed on obtaining a comprehensive and kinetically accurate model able to predict a wide variety of H_2–CO combustion data. The model was subject to systematic optimization and validation tests against reliable H_2–CO combustion data, from global combustion properties (shock-tube ignition delays, laminar flame speeds, and extinction strain rates) to detailed species profiles during H_2 and CO oxidation in flow reactor and in laminar premixed flames.

Keywords: Kinetics; Detailed reaction model; Hydrogen; Carbon monoxide

1. Introduction

The most successful model of H_2–CO combustion has been that of Mueller et al. [1], developed on the basis of a careful evaluation of relevant kinetic parameters and flow reactor experiments. The model is also able to predict a wide range of flame experiments. Over the last few years, however, the rate parameters of the key reaction $H + O_2 + M = HO_2 + M$ and its third-body efficiencies have been revised [2,3], giving an urgent reason for a re-examination of the H_2–CO combustion model. The downward revision of the enthalpy of formation of OH [4] may also exert an influence on the overall reaction kinetics of H_2 combustion.

Several new studies [5–7] have been reported in recent years. Two of these studies analyzed the hydrogen submodel [5,6], both being an extension of the model of Mueller et al. The third analysis [7] considered both H_2 and CO chemistry and is the predecessor to the present study. The objectives of the present study are (1) to provide an update for the H_2–CO combustion reaction model on the basis of recent kinetic data, and (2) to optimize the H_2–CO model against available H_2–CO combustion data.

2. Reaction model

The unoptimized (trial) reaction model consists of 14 species and 30 reactions as shown in Fig. 1. The model and its thermochemistry and transport property files can be found at the URL: http://ignis.me.udel.edu/h2co. The trial model was based on a careful review of recent kinetics literature, considering both direct data and compilations. A large number of GRI 3.0 rate parameters [8] were

* Corresponding author. Present address: Exponent, 21 Strathmore Road, Natick, MA 01760, USA. Fax: +1 508 647 3619.
E-mail address: daviss@exponent.com (S.G. Davis).

1540-7489/$ - see front matter © 2004 The Combustion Institute. Published by Elsevier Inc. All rights reserved.
doi:10.1016/j.proci.2004.08.252

no.	reaction	rate parameters[a] $A^{(b)}$	n	E	f^c	ref/ comments[c]
1	H+O$_2$=O+OH	2.65(16)	−0.671	17041	1.15	[8]
2	O+H$_2$=H+OH	3.87(04)	2.7	6260	1.3	[8]
3	OH+H$_2$=H+H$_2$O	2.16(08)	1.51	3430	1.3	[8]
4	2OH=O+H$_2$O	3.57(04)	2.4	−2110	1.3	[8]
5	2H+M=H$_2$+M	1.00(18)	−1		2	[8]
5a	H$_2$O/60$T^{-0.25}$/ H$_2$/0.05067$T^{-0.4}$/, CO/1/, CO$_2$/309T^{-1}/, Ar/0.63/, He/0.63/				2	*d*
6	H+OH+M=H$_2$O+M	2.20(22)	−2		2	[8]
	H$_2$/2/, H$_2$O/6.3/, CO/1.75/, CO$_2$/3.6/, Ar/0.38/, He/0.38/					
7	O+H+M=OH+M	4.71(18)	−1		2	[9]
	H$_2$/2/, H$_2$O/12/, CO/1.75/, CO$_2$/3.6/, Ar/0.7/, He/0.7/					
8	2O+M=O$_2$+M	1.20(17)	−1			[8]
	H$_2$/2.4/, H$_2$O/15.4/, CO/1.75/, CO$_2$/3.6/, Ar/0.83/, He/0.83/					
9	H+O$_2$(+M) =HO$_2$(+M)	4.65(12)	0.44		1.2	[2], k_∞
		5.75(19)	−1.4		1.2	k_0, *e*
9a	Ar/0.53/				1.2	*d*
9b	He/0.53/				1.2	*d*
9c	O$_2$/0.75/				1.2	*d*
9d	H$_2$O/12/				1.2	*d*
9e	H$_2$/1.0/ CO/1.2/, CO$_2$/2.4/				1.2	*d*
10	H$_2$+O$_2$=HO$_2$+H	7.40(05)	2.433	53502	1.25	[10]
11	2OH(+M) =H$_2$O$_2$(+M)	7.40(13)	−0.37		1.5	[11], k_∞
		1.34(17)	−0.584	−2293	1.5	k_0, *f*
	H$_2$/2/, H$_2$O/6/, CO/1.75/, CO$_2$/3.6/, Ar/0.7/, He/0.7/					
12	HO$_2$+H=O+H$_2$O	3.97(12)		671		[8]
13	HO$_2$+H=OH+OH	7.08(13)		295	2	[13]
14	HO$_2$+O=OH+O$_2$	2.00(13)			2	[8]
15a	HO$_2$+OH=O$_2$+H$_2$O	2.90(13)		−500	2	[14]
15b		1.00(16)		17330		[15]
16a	2HO$_2$=O$_2$+H$_2$O$_2$	1.30(11)		−1630		[16]
16b		4.20(14)		12000	1.5	[16]
17	H$_2$O$_2$+H=HO$_2$+H$_2$	1.21(07)		25200	2	[8]
18	H$_2$O$_2$+H=OH+H$_2$O	2.41(13)		3970		[9]
19	H$_2$O$_2$+O=OH+HO$_2$	9.63(06)		23970		[9]
20a	H$_2$O$_2$+OH=HO$_2$+H$_2$O	2.00(12)		427		[15]
20b		2.67(41)		−737600		*g*
21	CO+O(+M) =CO$_2$(+M)	1.80(10)		2384	2	[13],k_∞
		1.55(24)	−2.79	4191	2	k_0, *h*
	H$_2$/2/, H$_2$O/12/, CO/1.75/, CO$_2$/3.6/, Ar/0.7/, He/0.7/					
22a	CO+OH=CO$_2$+H	9.60(11)	0.14	7352	1.2	*i*
22b		7.32(10)	0.03	−16	1.2	*i*
23	CO+O$_2$=CO$_2$+O	2.53(12)		47700	3	[9]
24	CO+HO$_2$=CO$_2$+OH	3.01(13)		23000	2	[1]
25	HCO+H=CO+H$_2$	1.20(14)			2	[17]
26	HCO+O=CO+OH	3.00(13)				[8]
27	HCO+O=CO$_2$+H	3.00(13)				[8]
28	HCO+OH=CO+H$_2$O	3.02(13)				[9]
29	HCO+M=CO+H+M	9.35(16)	−1	17000	2	[17]
29a	H$_2$O/12/ H$_2$/2/, CO/1.75/, CO$_2$/3.6/, Ar/1/, He/1/				2	*d*
30	HCO+O$_2$=CO+HO$_2$	1.20(10)	0.807	−727		[18]

[a] Rate parameters $k=AT^n\exp(-E/RT)$. Units are cm, s, mol, and cal. Unless otherwise indicated, multiple entries of rate expressions for a reaction indicate the rate coefficient is the sum of these expressions. [b] The number in the parenthesis is the exponent of 10, i.e., 2.65(16) = 2.65×10^{16}. Parameters highlighted in red are active and subject to optimization. [c] f is the uncertainty factor or span assigned to active A factors. [d] The third-body collision efficiency is active and subject to optimization. [e] Center broadening factor $F_c = 0.5$. [f] Low-pressure limit fit to expressions given in [11] and [12]. $F_c = 0.2654\exp(-T/1756) + 0.7346\exp(-T/5182)$. [g] Fit to the expression of [16]. [h] $F_c = 1$ (Lindemann fall-off). [i] This work (see text).

Fig. 1. Trial reaction model of H_2–CO oxidation, active parameters, and their spans employed in model optimization (see Refs. [9,14,16–18]).

found to be appropriate and are used. The discussion below highlights the choice of key rate parameters.

The rate expression of $H + O_2 = O + OH$ was taken from GRI 3.0 [8]. The rate coefficient of $H + O_2(+M) = HO_2(+M)$ was based on Troe [2], who employed a high-pressure rate $k_{rec,\infty}$ (cm^3 mol^{-1} s^{-1}) $= 4.65 \times 10^{12} T^{0.44}$ and developed the low-pressure and fall-off expressions for Ar and N_2 as the bath gases. The broadening factor F_c was found to be 0.5 for both third bodies. Troe's fall-off rate parameterization, however, could not be directly used in CHEMKIN [19], because the low-pressure limit rate coefficient k_0 does not share the same temperature dependence for different third bodies. We had to develop parameterized rate expressions (see Fig. 1) based on the k_0 expression of Ar and using the fall-off formula of Troe [20]. A collision efficiency factor $\beta = 0.53$ was used for Ar relative to N_2. The collision efficiency of He was assumed to be equal to that of Ar. The study of Michael et al. [3] supports a collision efficiency of O_2 smaller than that of N_2. We found that for O_2, $\beta = 0.75$ gives a good agreement with experiment [3] and theory [2]. For H_2O, Troe [2] suggested that the broadening factor is close to the strong-collision limit. We chose a β value of 12 (relative to N_2) with the resulting rate in good agreement with those of Troe and others [2,3,21].

The k_0 expression of $H + OH + M = H_2O + M$ was taken from [8] with the β values equal to 0.38 and 6.3 for Ar and H_2O, respectively [12]. The rate expression of Michael et al. [10] was employed for $H_2 + O_2 = H + HO_2$. For $OH + OH(+M) = H_2O_2(+M)$, the k_0 expression, given in the reverse direction by Baulch et al. [12], was refitted based on the new heat of formation of the OH radical along with the low temperature data of Zellner et al. [11]. The $k_{rec,\infty}$ expression and the β value of H_2O (6) were taken from [11] while the Troe fall-off parameters [22] were the same as those in GRI 3.0. The rate expressions for $H_2O_2 + OH = HO_2 + H_2O$ were taken directly from [15], though the high-temperature expression was refitted using a modified Arrhenius expression to avoid the rate constant values exceeding the collision limit when extrapolated to high temperatures.

For $CO + O(+M) = CO_2(+M)$, the k_∞ expression was taken from [13], and following Allen et al. [23], k_0 was taken from the QRRK analysis of Westmoreland et al. [24] and fall-off was that of Lindemann. The collision efficiency of H_2O was assumed to be 12. The rate constant for $CO + OH = CO_2 + H$ was re-analyzed in the present study, and the experimental data were refitted by the sum of two modified Arrhenius expressions. The new expression resolves more accurately the high temperature data of Wooldridge et al. [25] as well as the data found in [26]. Without this revision, it was not possible to reconcile the high-temperature H_2 ignition data with the H_2–CO laminar flame speeds. The known pressure dependence of this reaction was not considered as this dependence is quite unimportant for the CO oxidation experiments considered herein.

3. Computational and optimization method

A comprehensive review was conducted for a large number of H_2–CO combustion data. Thirty-six experiments were chosen as optimization targets as shown in Table 1. They can be classified into four categories: (1) laminar flame speeds of H_2–air, H_2–O_2–He, and H_2–CO–air mixtures, (2) the peak mole fractions of H and O in a low-pressure burner-stabilized H_2–O_2–Ar flame, (3) the consumption rates of H_2 and CO during the reaction of H_2–O_2–N_2 and CO–O_2–H_2O–N_2 mixtures in a turbulent flow reactor, and (4) ignition delay times of H_2–O_2–Ar and H_2–CO–O_2–Ar mixtures behind reflected shock waves.

Ignition delay and flow reactor calculations were conducted using a kinetic integrator interfaced with CHEMKIN [19] by assuming adiabatic condition. Ignition delays were modeled using the constant-density model, whereas flow reactor modeling used the constant-pressure assumption. The numerical ignition delays were determined following the same ignition criteria as in the respective experiments. Laminar flame speeds and structure were calculated using Premix [40], employing thermal diffusion, and multicomponent transport. Diffusion coefficients of several key pairs were updated [41].

Sensitivity analyses were conducted for ignition delay and consumption rates of the fuel in flow reactor with a brute force method. For laminar flame speeds and H and O peak mole fractions in burner-stabilized flames, the local sensitivity methods were utilized. Based on the sensitivity information, active rate parameters (to be optimized) were chosen for each target. The entire set of active parameters consists of 28 A-factors and third-body efficiency factors as shown in Figs. 1 and 2.

The optimization approach is similar to earlier studies [8,43]. Briefly, the solution mapping technique was employed to express a response by a second-order polynomial $\eta^{(2)} = a_0 + \sum_{j=1}^{n} a_i x_i + \sum_{i=1}^{n} \sum_{j \geqslant i}^{n} b_{ij} x_i x_j$, where a's and b's are the coefficients, x's are factorial active variables given by $x = \ln(\alpha/\alpha_{\text{trial}})/\ln(f)$, where α is the active A factor or third-body efficiency factor, and f is its span or uncertainty factor. The uncertainty factor was estimated on the basis of kinetic uncertainty and is provided in Fig. 1 for each active parameter. Though an optimization of the temperature dependence of rate coefficients is possible, we chose not to vary the T-dependence because of the insufficient number of systematic experimental targets [43].

For flow reactor targets, the response was found to be highly non-linear with respect to x's. These responses are expressed by adding a hyperbolic tangent term to account for the S-shaped dependence of response with respect to x's, $\eta = \eta^{(2)} + c \tanh(a'_0 + \sum_{j=1}^{n} a'_i x_i + \sum_{i=1}^{n} \sum_{j \geqslant i}^{n} b'_{ij} x_i x_j)$. The coefficients for the flow reactor and ignition delay targets were calculated by a factorial design test [43]. The coefficients for flame targets were obtained using the sensitivity analysis based method [44].

Minimization was carried out on the objective function $L^2 = \Sigma_i[(\eta_{i,\text{expt}} - \eta_{i,\text{calc}})/\sigma_i]^2$ subject to the constraint $-1 < \{x\} < +1$, where the subscript i denotes the ith target. Each target was individually weighted by their uncertainty σ_i. The target values and their uncertainties are presented in Table 1.

4. Results and discussion

The trial kinetic model was tested against a wide range of experimental data. The predictions of the trial model for the 36 target values are shown in Table 1 (the "trial" column). Overall the model performed well against these experimental data. The exceptions are: it overpredicts H_2–O_2–He flame speeds, the H and O mole fractions in the burner-stabilized flame, and the consumption rate of H_2 for the 1.0% H_2–1.5 O_2%–N_2 flow reactor mixture at 943 K and 2.5 atm.

To reconcile these discrepancies, optimization was then carried out for 28 active parameters with respect to 36 targets. All active parameters were allowed to vary freely within their uncertainty spans. The optimal parameter set was obtained as the minimum of L^2, first from a random sample of the multidimensional parameter space, followed by a Newton search of the L^2 minimum in the parameter space. The values of optimized active parameters are shown in the last column of Fig. 2 (expressed as the optimized-to-trial parameter ratio). To obtain the optimized model, the active parameters (A-factors and third-body efficiency factors) shown in Fig. 1 should be multiplied by their corresponding ratios.

Validation of the optimized model will be discussed below. Figure 3 presents experimental [27–31,45] and computed laminar flame speeds of H_2–air and air-equivalent mixtures where N_2 was replaced by Ar or He. With trial model predictions already close to the experimental values, the optimization served only to fine-tune the model, resulting in excellent agreement with the experiment as can be seen in Fig. 3 and Table 1. The trial model tends to overpredict the H_2–O_2–He flame speeds at elevated pressures (Table 1). The discrepancies are clearly caused by kinetics as a previous study showed that the uncertainty in the transport coefficients cannot account for the observed differences [41]. Now the optimized model can successfully predict these H_2–O_2–He flame speeds [27] as seen in Fig. 4. This agreement was brought by lowering the rate of $OH + H_2 = H + H_2O$, $H + HO_2 = OH + OH$, and a small increase in the rate of $H + O_2 + H_2O = HO_2 + H_2O$.

The dominant sensitivity of the laminar flame speeds of H_2–CO–air mixtures, especially the

Table 1
Optimization targets

Target No.	Composition (mol %)					$T_0(T_5)$ (K)	$p_0(p_5)$ (atm)	Comments	Target		Model		Units
	H_2	O_2	CO	H_2O	Diluent				Value $\pm \sigma$	Ref.	Trial	Opt.	
Flame speed													
fls 1a	29.6	14.8	—	—	N_2	298.2	1	H_2–air, $\phi = 1$	204 ± 20	[27–31]	221	206	cm/s
fls 1b	55.8	9.3	—	—	N_2	298.2	1	H_2–air, $\phi = 3$	217 ± 20	[27,28,31]	228	216	cm/s
fls 2a	20	10	—	—	He	298.2	1	$\phi = 1$	206 ± 20	[27]	237	231	cm/s
fls 2b	36	8	—	—	He	298.2	1	$\phi = 2.25$	249 ± 25	[27]	265	258	cm/s
fls 3a	13.8	6.9	—	—	He	298.2	15	$\phi = 1$	58 ± 6	[27]	69	61	cm/s
fls 3b	21.9	6.3	—	—	He	298.2	15	$\phi = 1.75$	88 ± 9	[27]	97	91	cm/s
fls 4a	1.6	14.2	30.9	—	N_2	298.2	1	$\phi = 1.148$	40 ± 4	[32]	42	42	cm/s
fls 4b	3	8	59	—	N_2	298.2	1	$\phi = 3.895$	52.5 ± 5	[32]	56	53	cm/s
fls 5a	14.8	14.8	14.8	—	N_2	298.2	1	$\phi = 1$	111.5 ± 11	[32]	114	110	cm/s
fls 5b	28.1	9.2	28.1	—	N_2	298.2	1	$\phi = 3.05$	154.5 ± 15	[32]	161	155	cm/s
fls 6a	9.2	17.4	7.8	—	N_2	298.2	1	$CO/H_2 = 0.84$	10.3 ± 2.0	[33]	11	11	cm/s
fls 6b	2.9	17.4	14.1	—	N_2	298.2	1	$CO/H_2 = 4.90$	18.5 ± 2.0	[33]	20	20	cm/s
Flat flame													
flf 1a	39.7	10.3	—	—	Ar	—	0.047	$x_{H,max}$	0.067 ± 0.051	[34]	0.103	0.077	—
flf 1b	39.7	10.3	—	—	Ar	—	0.047	$x_{O,max}$	0.002 ± 0.015	[34]	0.003	0.003	—
Flow reactor													
flw 1a	1.18	0.61		—	N_2	914	15.7	a	8.6 ± 0.5	[13]	10.4	8.7	ppm/ms
flw 2a	1.01	0.52	—	—	N_2	935	6	a	13.0 ± 0.5	[13]	11.2	12.4	ppm/ms
flw 3a	1.0	1.5	—	—	N_2	943	2.5	a	98 ± 10	[13]	532	97	ppm/ms
flw 4a	0.5	0.5	—	—	N_2	880	0.3	a	261 ± 20	[13]	334	318	ppm/ms
flw 5a	—	0.517	1.014	0.65	N_2	1038	1	b	354 ± 40	[35]	293	282	ppm/ms
flw 6a	—	0.494	0.988	0.65	N_2	1038	3.46	b	140 ± 20	[35]	54	53	ppm/ms
flw 6b	—	0.494	0.988	0.65	N_2	1038	3.46	c	229 ± 20	[35]	242	237	ms
flw 7a	—	0.482	1.002	0.65	N_2	1068	6.5	d	14.1 ± 0.5	[35]	19.0	14.6	ppm/ms
flw 8a	0.95	0.49	—	—	N_2	934	3.02	e	19.0 ± 1.0	[13]	17.8	19.0	ppm/ms
flw 8b	0.95	0.49	—	—	N_2	934	3.02	f	70 ± 5	[13]	62	68	ms
Shock-tube ignition													
ign 1a	6.67	3.33	—	—	Ar	1051	1.729	Onset of p rise	231 ± 120	[36]	320	310	μs
ign 1b	6.67	3.33	—	—	Ar	1312	2.008		50 ± 25	[36]	62	62	μs
ign 2a	20	10	—	—	Ar	1033	0.518	Maximum p	238 ± 140	[37]	345	342	μs
ign 2b	20	10	—	—	Ar	1510	0.493		29 ± 20	[37]	37	39	μs
ign 3a	0.5	0.25	—	—	Ar	1754	33	Maximum [OH]	10 ± 3	[38]	11	11	μs
ign 4a	2	1	—	—	Ar	1189	33	Maximum [OH]	293 ± 100	[38]	243	168	μs
ign 4b	2	1	—	—	Ar	1300	33		11 ± 4	[38]	24	20	μs
ign 5a	0.1	0.05	—	—	Ar	1524	64	Maximum [OH]	54 ± 25	[38]	64	60	μs
ign 6a	0.05	1	12.17	—	Ar	2160	1.492	Onset of CO_2 rise	63 ± 25	[39]	56	60	μs
ign 6b	0.05	1	12.17	—	Ar	2160	1.492	$[O] = 2.5 \times 10^{14}$ cm^{-3}	47 ± 25	[39]	34	41	μs
ign 6c	0.05	1	12.17	—	Ar	2625	1.949	Onset of CO_2 rise	23 ± 10	[39]	20	22	μs
ign 6d	0.05	1	12.17	—	Ar	2625	1.949	$[O] = 2.5 \times 10^{14}$ cm^{-3}	11 ± 6	[39]	10	13	μs

[a] The target value is $\Delta x_{H_2}/\Delta t|^{0.6}_{c_{H_2}=0.4}$, where x is the mole fraction (ppm); c is the fractional conversion.
[b] $\Delta x_{CO}/\Delta t|^{0.6}_{c_{CO}=0.4}$.
[c] $\Delta t|^{0.95}_{c_{CO}=0.75}$.
[d] $\Delta x_{CO}/\Delta t|^{0.6}_{c_{CO}=0.4}$.
[e] $\Delta x_{CO}/\Delta t|^{0.95}_{c_{H_2}=0.85}$.
[f] $\Delta t|^{0.9}_{c_{H_2}=0.4}$.

	fls												flf		flw										ign												
no.	1a	1b	2a	2b	3a	3b	4a	4b	5a	5b	6a	6b	1a	1b	1a	2a	3a	4a	5a	6a	6b	7a	8a	8b	1a	1b	2a	2b	3A	4a	4b	5a	6a	6b	6c	6d	$\alpha_{opt}/\alpha_{trial}$ [a]
1	x	x	x	x	x	x	x	x	x	x	x	x	x	x	x	x	x	x	x	x	x	x	x	x	x	x	x	x	x	x	x	x	x	x	x	x	1
2	x	x	x	x	x	x	x	x	x	x	x	x		x	x	x	x	x		x	x		x	x	x	x	x	x	x	x	x	x	x	x	x	x	1.19
3	x	x	x	x	x	x	x	x	x	x	x			x	x	x	x	x	x				x	x	x	x	x	x	x	x	x	x		x			0.8
4							x				x								x	x	x	x													x		1.11
5		x		x		x		x		x			x						x													x					1.78
5a	x	x	x	x	x	x				x			x	x										x													0.94
6	x	x	x	x	x	x	x	x	x	x	x	x	x	x					x							x		x	x			x					2*
7	x				x	x	x		x	x			x	x				x								x		x									2*
9		x					x		x		x	x	x	x	x	x	x	x	x	x	x	x	x	x													1.1
9a													x	x											x		x		x	x	x	x					0.83*
9b			x	x	x	x																															0.95
9c											x	x	x	x											x												1.25*
9d	x	x	x	x	x	x			x		x	x	x	x		x	x	x		x	x	x				x											1.09
9e		x		x		x							x	x	x										x		x			x	x						0.83
10	x	x	x	x	x	x	x	x	x	x	x	x	x	x	x	x	x	x	x	x	x	x	x	x	x	x	x	x	x	x		x	x	x	x	x	0.8*
11															x	x	x						x	x						x							1.5*
13	x	x	x	x	x	x	x	x	x	x	x	x	x	x	x	x	x	x	x	x	x	x	x	x	x	x	x		x	x	x	x					1.06
14					x						x	x			x	x	x		x	x	x	x	x	x													2*
15a	x	x	x	x	x	x	x	x	x	x	x	x			x	x	x		x	x	x	x	x	x							x	x					0.82
16b															x	x	x	x			x	x															0.87
17															x				x											x	x	x					0.5*
21								x			x								x	x	x	x											x	x	x		0.76
22a							x	x	x	x	x	x							x	x	x	x											x	x	x	x	0.83*
22b							x	x	x	x	x	x							x	x	x	x											x	x	x		1.2*
23																																	x	x	x	x	0.44
25								x		x																											1
29								x		x																											2*
29a										x																											2*

[a] α is the active *A* factor or third-body efficiency factor. The asterisk (*) indicates that the optimized parameter lies on the boundary of the span

Fig. 2. Target-active parameter matrix.

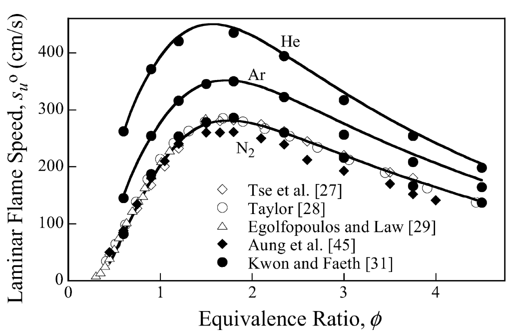

Fig. 3. Experimental (symbols) and computed (lines: the optimized model) H_2–air and air equivalent (N_2 is replaced by Ar or He) flame speed at a pressure of 1 atm.

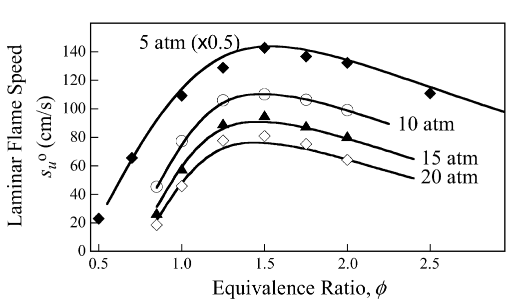

Fig. 4. Experimental (symbols [27]) and computed (lines: the optimized model) H_2–O_2–He flame speeds.

95% CO + 5% H_2 mixtures, to $CO + OH = CO_2 + H$ has been observed elsewhere [32] and necessitated a re-evaluation this reaction. It was determined that the sum of two modified Arrhenius expressions was necessary to predict the laminar flame speed data. Figures 5 and 6 show that the optimized model reproduces experimental H_2–CO–air laminar flame speeds [32,33].

Figure 7 depicts species profiles for four selected H_2 oxidation experiments in a turbulent flow reactor [13]. Time shift was necessary to match the computed profiles with the experimental counterparts. The amounts of time shift were found to be similar with those used by Mueller et al. [13]. It is seen that the optimized model predicts the experimental species profile accurately, and it also improved the prediction of the experiment as compared to the trial model (cf. Fig. 7B). Similarly, the results of Fig. 8 show that for CO oxidation [35] the optimized model accurately predicts the CO consumption rate over an extended pressure range.

The trial model could accurately reconcile most of the ignition delay data for H_2–O_2–diluent mixtures, and optimization served only to improve these predictions as can be seen in Table 1. In addition, Fig. 9 shows a plot of experimental and computed ignition delay times for H_2–O_2–Ar mixtures [36–38,46] behind reflected shock waves. Here, the experimental shock-tube ignition delay data were fitted into $\tau\ (\mu s) = [H_2]^{-0.154}[O_2]^{-0.693}[Ar]^{0.04}\ [6.77\times10^{-8}\,T^{0.252}e^{9234/T}]$ for non-"run-

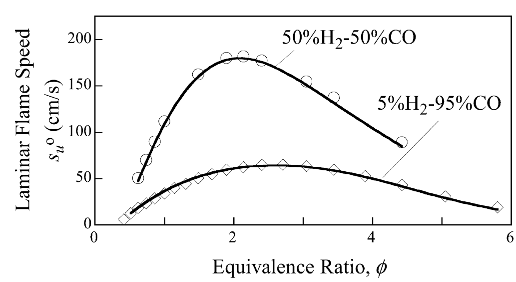

Fig. 5. Experimental (symbols [32]) and computed (lines: the optimized model) H_2–CO–air flame speeds at a pressure of 1 atm.

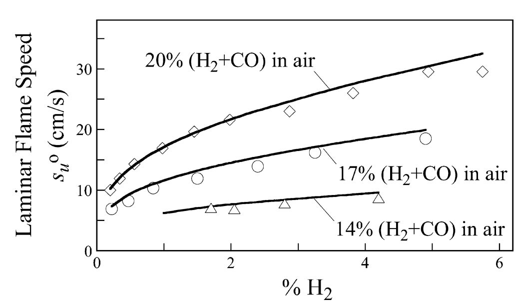

Fig. 6. Experimental (symbols [33]) and computed (lines: the optimized model) H_2–CO–air flame speeds at a pressure of 1 atm.

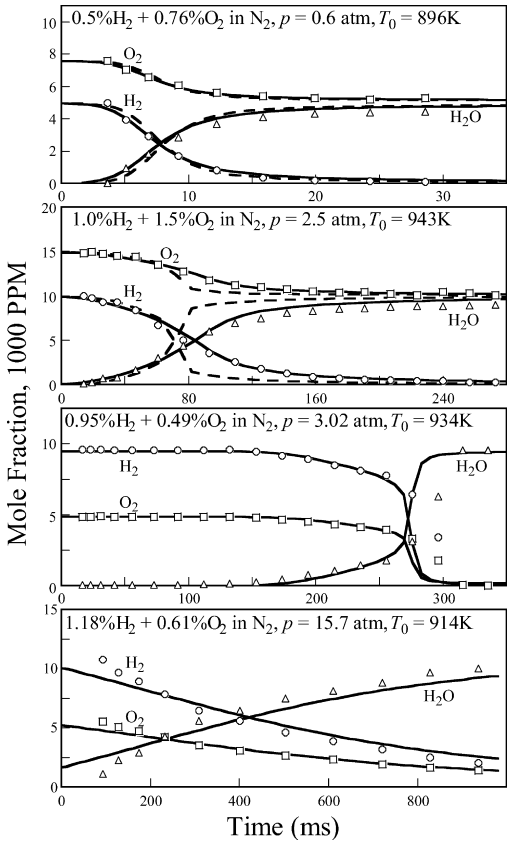

Fig. 7. Experimental (symbols [13]) and computed (lines) species mole fraction profiles during hydrogen oxidation in a flow reactor. Solid lines: optimized model; dashed lines: trial model.

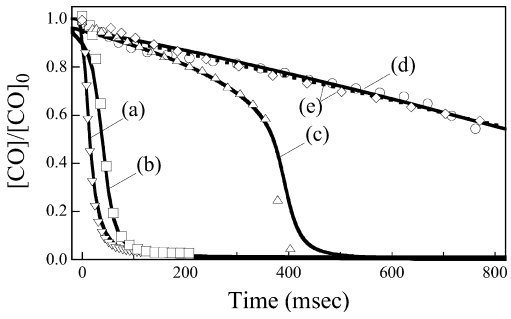

Fig. 8. Experimental (symbols [35]) and computed (lines) $[CO]/[CO]_0$ profiles during moist CO oxidation in a flow reactor. Cases (a): 1.014% CO + 0.517% O_2 + 0.65% H_2O in N_2, $p = 1$ atm, $T_0 = 1038$ K, (b) 1.01% CO + 0.496% O_2 + 0.65% H_2O in N_2, $p = 2.44$ atm, $T_0 = 1038$ K, (c) 0.988% CO + 0.494% O_2 + 0.65% H_2O in N_2, $p = 3.46$ atm, $T_0 = 1038$ K, (d) 0.984% CO + 0.497% O_2 + 0.65% H_2O in N_2, $p = 6.5$ atm, $T_0 = 1040$ K, and (e) 0.994% CO + 1.47% O_2 + 0.65% H_2O in N_2, $p = 9.6$ atm, $T_0 = 1039$ K.

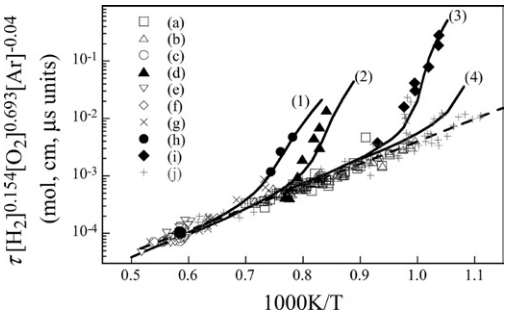

Fig. 9. Experimental (symbols) and computed (lines) ignition delay times of H_2–O_2–Ar mixtures behind reflected shock waves. Symbols: (a) 6.67% H_2 + 3.33% O_2, $p_5 = 1.35$–2.90 atm; (b) 5% H_2 + 5% O_2, $p_5 = 1.35$–2.90 atm (onset of pressure rise [36]), (c) 0.5% H_2 + 0.25% O_2, $p_5 = 33$ atm, (d) 2% H_2 + 1% O_2, $p_5 = 33$ atm, (e) 0.5% H_2 + 0.25% O_2, $p_5 = 57$ atm, (f) 0.33% H_2 + 0.17% O_2, $p_5 = 64$ atm, (g) 0.1% H_2 + 0.05% O_2, $p_5 = 64$ atm, (h) 0.5% H_2 + 0.25% O_2, $p_5 = 87$ atm (maximum OH absorption rate [38]), (i) 8% H_2 + 2% O_2, $p_5 = 5$ atm (maximum OH emission) [46], and (j) four $H_2 + O_2$ mixtures [37]. Lines: (1) 0.5% H_2 + 0.25% O_2, $p_5 = 87$ atm (maximum [OH] rate), (2) 2% H_2 + 1% O_2, $p_5 = 33$ atm (maximum [OH] rate), (3) 8% H_2 + 2% O_2, $p_5 = 5$ atm (maximum [OH]), and (4) 5% H_2 + 5% O_2, $p_5 = 2$ atm (maximum pressure gradient).

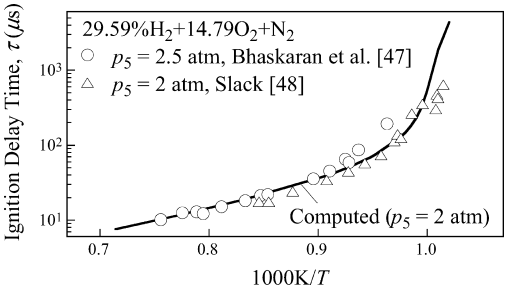

Fig. 10. Experimental (symbols) and computed (lines) ignition delay times behind reflected shock waves for H_2–O_2–N_2 mixtures. Experimental data were determined from onset of pressure rise [47] and maximum rate of OH emission [48].

away" data, i.e., those fall on the nearly linear portion of the curves of Fig. 9, where [ ] denotes concentration in mol/cm^3. For mixtures of H_2–O_2–N_2 [47,48], comparison was also made as seen in Fig. 10, where the result should only be considered as a secondary validation because the vibrational relaxation of N_2 was not accounted for in modeling. The optimized model also predicts fairly well the ignition delay of CO-H_2–O_2–Ar mixtures [39] as seen in Fig. 11.

The optimized model resulted in improved prediction of the species profiles measured in a low-pressure H_2–O_2–Ar flame, though the concen-

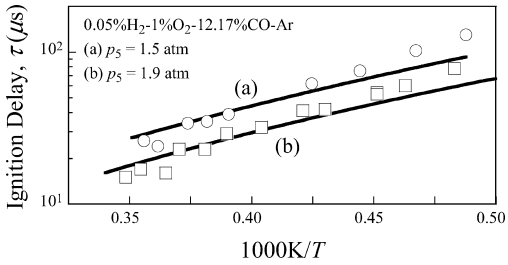

Fig. 11. Experimental (symbols [39]) and computed (lines) ignition delay times behind reflected shock waves. The experimental ignition delay was determined from the onset of infrared emission due to CO_2; the computational ignition delay determined from the maximum CO_2 concentration gradient.

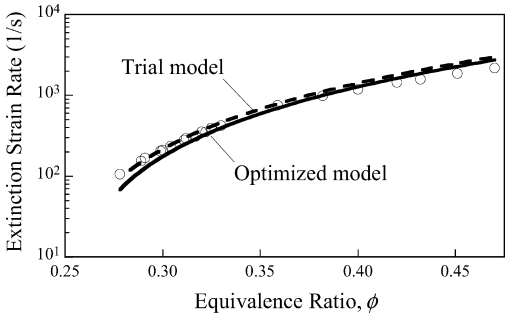

Fig. 12. Experimental (symbols [42]) and computed (lines) extinction strain rates as a function of the equivalence ratio for ultra-lean H_2–air mixtures.

trations of H and O are still overpredicted (see, Table 1). These discrepancies may well be caused by the experimental uncertainty due to flame perturbation by the sample probe.

Finally, the trial model (dashed lines) and the optimized model (solid lines) were compared against extinction strain rates of ultra-lean H_2–air mixtures [42]. These experiments were not used as optimization targets because of large influences from the uncertainties in the diffusion coefficients. The results of Fig. 12 indicate that both the trial and optimized model can accurately predict the data for the leaner equivalence ratios, and begin to deviate as the equivalence ratio approaches 0.5. Again, this deviation may be due to diffusion effects and shows the need to include diffuse coefficients in the optimization space [42].

The optimization procedure also allows us to probe the residual kinetic uncertainties. We found that the rate coefficient of $H + O_2 = OH + O$ always stayed within 5% of the trial value for all optimization runs made, including the use of a smaller number of targets and/or a reduced dimensionality of active parameter space. The rate coefficient is within 8% and 20% from the analysis of Troe and Ushakov [49] for $T > 1500$ and 1000 K, respectively. Again, our assignment of rate constant uncertainties prior to optimization is consistent with these differences. Of the remaining active parameters, the optimized k_2, k_3, and k_4 values are often within 20% of the trial values. For $H + O_2(+M) = HO_2(+M)$, optimization led to a 10% increase in the rate coefficient of the base reaction ($M = N_2$), which is acceptable. For $M = H_2O$, the optimized third-body efficiency was a factor of 1.09 of the trial value. Coupled with the change in the rate for base reaction ($M = N_2$), the third-body efficiency of H_2O relative to N_2 remains unchanged. Optimization yielded a smaller efficiency factor for argon, driven primarily by the ignition delay data (the trial model overpredicts ignition delays). The resulting efficiency factor is equal to 0.46 (relative to N_2), and the corresponding rate coefficient for $H + O_2 + Ar = HO_2 + Ar$ is within the experimental uncertainty given in [10]. The low-temperature rate coefficient of $HO_2 + OH = HO_2 + OH$ and the high-temperature rate of $HO_2 + HO_2 = O_2 + H_2O_2$ were lowered by 18% and 13% upon optimization, respectively. Both give a better agreement with the rates recommended by Troe and Ushakov [49].

Among the 28 active parameters, 12 "hit" their respective boundaries of uncertainty spans. The fraction of these parameters is much smaller than what is usually encountered in kinetic model optimization (see, for example [50]). Some of these parameters are either inadequately constrained because of a lack of relevant targets or because they are only marginally active for H_2–CO combustion (e.g., 9c, 9e, 23, 25, 29, and 29a). Others may be caused by target data inconsistency [51]. These issues, while worthy to explore, are clearly outside of the scope of the present study.

5. Summary

A H_2–CO kinetic model was proposed. The model was based on a comprehensive review of literature kinetic data, considering the recent revisions in the rate coefficient of $H + O_2(+M) = HO_2(+M)$, its third-body efficiencies, and the enthalpy of formation of the OH radical. The trial model performed very well against most of the H_2/CO combustion data. Discrepancies in the predictions, however, existed for several data sets. These discrepancies were successfully resolved by optimization within the uncertainty bounds of the relevant rate parameters with respect to 36 targets, including the global combustion properties of ignition delays and laminar flame speeds, and the detailed species profiles during H_2 and CO oxidation in flames and flow reactors. It is shown that this set of H_2–CO combustion targets can be reconciled within the underlying kinetic uncertain-

ties, and the optimized kinetic model is predictive for all reliable H_2–CO combustion data considered herein.

Acknowledgments

This work was supported by AFOSR (Grant Nos. F49620011014 and F496200210002) under the technical supervision of Dr. Julian M. Tishkoff. The work at UD was also supported by NSF (CTS-9874768).

References

[1] M.A. Mueller, R.A. Yetter, F.L. Dryer, *Int. J. Chem. Kinet.* 31 (1999) 705–724.
[2] J. Troe, *Proc. Combust. Inst.* 28 (2000) 1463–1469.
[3] J.V. Michael, M.-C. Su, J.W. Sutherland, J.J. Carroll, A.F. Wagner, *J. Phys. Chem. A* 106 (2002) 5297–5313.
[4] B. Ruscic, D. Feller, D.A. Dixon, K.A. Peterson, L.B. Harding, R.L. Asher, A.F. Wagner, *J. Phys. Chem. A* 105 (2001) 1–4.
[5] H. Curran, Personal communication, 2003.
[6] J. Li, Z. Zhao, A. Kazakov, D.L. Dryer, An updated comprehensive kinetics model of H_2 combustion, in: *Chemical and Physical Processes in Combustion, the 2003 Technical Meeting of the Eastern States Section of the Combustion Institute*. University Park, PA, October 2003, pp. 169–171.
[7] S.G. Davis, A.V. Joshi, H. Wang, F.N. Egolfopoulos, A comprehensive and optimized kinetic model of H_2/CO combustion, in: *Proceedings of the 3rd Joint Meeting of the U.S. Sections of the Combustion Institute*. Chicago, March 2003, paper PK8.
[8] G.P. Smith, et al. GRI-Mech 3.0. Available from: <http://www.me.berkeley.edu/gri_mech/> (2000).
[9] W. Tsang, R.F. Hampson, *J. Phys. Chem. Ref. Data* 15 (1986) 1087–1279.
[10] J.V. Michael, J.W. Sutherland, L.B. Harding, A.F. Wagner, *Proc. Combust. Inst.* 28 (2000) 1471–1478.
[11] R.E. Zellner, F. Ewig, R. Paschke, Gg. Wagner, *J. Phys. Chem.* 92 (1988) 4184–4190.
[12] D.L. Baulch, C.J. Cobos, R.A. Cox, P. Frank, G. Hayman, T. Just, J.A. Kerr, T. Murrells, M.J. Pilling, J. Troe, R.W. Walker, J. Warnatz, *J. Phys. Chem. Ref. Data* 21 (1992) 411–734.
[13] M.A. Mueller, T.J. Kim, R.A. Yetter, F.L. Dryer, *Int. J. Chem. Kinet.* 31 (1999) 113–125.
[14] L.F. Keyser, *J. Phys. Chem.* 92 (1988) 1193–1200.
[15] H. Hippler, H. Neunaber, J. Troe, *J. Chem. Phys.* 103 (1995) 3510–3516.
[16] H. Hippler, J. Troe, J. Willner, *J. Chem. Phys.* 93 (1990) 1755–1760.
[17] G. Friedrichs, D.F. Davidson, R.K. Hanson, *Int. J. Chem. Kinet.* 34 (2002) 374–386.
[18] C.-C. Hsu, A.M. Mebel, M.C. Lin, *J. Phys. Chem.* 105 (1996) 2346–2352.
[19] R.J. Kee, J.A. Miller, T.H. Jefferson, *CHEMKIN: A general-purpose, problem-independent, transportable, Fortran chemical kinetics code package*, Technical Report SAND80-8003. Sandia National Laboratories, 1980.
[20] R.G. Gilbert, K. Luther, J. Troe, *Ber. Bunsenges Phys. Chem.* 87 (1983) 169–177.
[21] P.J. Ashman, B.S. Haynes, *Proc. Combust. Inst.* 27 (1998) 185–191.
[22] J. Troe, *Proc. Combust. Inst.* 15 (1975) 667–680.
[23] M.T. Allen, R.A. Yetter, F.L. Dryer, *Combust. Flame* 109 (1997) 449–470.
[24] P.R. Westmoreland, J.B. Howard, J.P. Longwell, A.M. Dean, *AIChE J.* 32 (1986) 1971–1979.
[25] M.S. Wooldridge, R.K. Hanson, C.T. Bowman, *Proc. Combust. Inst.* 25 (1994) 741–748.
[26] D.M. Golden, G.P. Smith, A.B. McEwen, C.L. Yu, B. Eiteneer, M. Frenklach, G.L. Vaghjiani, A.R. Ravishankara, F.P. Tully, *J. Phys. Chem. A* 102 (1998) 8598–8606.
[27] S.D. Tse, D.L. Zhu, C.K. Law, *Proc. Combust. Inst.* 28 (2000) 1793–1800.
[28] M.W. Dowdy, D.B. Smith, S. Taylor, *Proc. Combust. Inst.* 23 (1990) 325–333.
[29] F.N. Egolfopoulos, C.K. Law, *Proc. Combust. Inst.* 23 (1990) 333–340.
[30] C.M. Vagelopoulos, F.N. Egolfopoulos, C.K. Law, *Proc. Combust. Inst.* 25 (1994) 1341–1347.
[31] O.C. Kwon, G.M. Faeth, *Combust. Flame* 124 (2001) 590–610.
[32] I.C. McLean, D.B. Smith, S.C. Taylor, *Proc. Combust. Inst.* 25 (1994) 749–757.
[33] C.M. Vagelopoulos, F.N. Egolfopoulos, *Proc. Combust. Inst.* 25 (1994) 1317–1323.
[34] J. Vandooren, J. Bian, *Proc. Combust. Inst.* 23 (1990) 341–346.
[35] T.J. Kim, R.A. Yetter, F. Dryer, *Proc. Combust. Inst.* 25 (1994) 759–766.
[36] R.K. Cheng, A.K. Oppenheim, *Combust. Flame* 58 (1984) 125–139.
[37] A. Cohen, J. Larsen, Report BRL 1386, 1967.
[38] E.L. Peterson, D.F. Davidson, M. Rohrig, R.K. Hanson, in: *20th International Symposium on Shock Waves*, 1996, pp. 941–946.
[39] A.M. Dean, D.C. Steiner, E.E. Wang, *Combust. Flame* 32 (1978) 73–83.
[40] R.J. Kee, J.F. Grcar, M.D. Smooke, J.A. Miller, *A Fortran program for modeling steady laminar one-dimensional premixed flames*. Sandia National Laboratory Report SAND85-8240 (1986).
[41] P. Middha, B. Yang, H. Wang, *Proc. Combust. Inst.* 29 (2002) 1361–1369.
[42] Y. Dong, A.T. Holley, M.G. Andac, F.N. Egolfopoulos, S.G. Davis, P. Middha, H. Wang, Experimental and numerical studies of extinction of premixed lean H_2/air flames, *2004 Spring Technical Meeting of the Western States of the Combustion Institute*. University of California at Davis, Davis, California, March, 2004, paper 04S-19.
[43] M. Frenklach, H. Wang, M.J. Rabinowitz, *Prog. Energy Combust. Sci.* 18 (1992) 47–73.
[44] S.G. Davis, A.B. Mhadeshwar, D.G. Vlachos, H. Wang, *Int. J. Chem. Kinet.* 36 (2003) 94–106.
[45] K.T. Aung, M.I. Hassan, G.M. Faeth, *Combust. Flame* 109 (1997) 1–24.
[46] G.B. Skinner, G.H. Ringrose, *J. Chem. Phys.* 42 (1965) 2190–2192.
[47] K.A. Bhaskaran, M.C. Gupta, T. Just, *Combust. Flame* 21 (1973) 45–48.
[48] M.W. Slack, *Combust. Flame* 28 (1977) 241–249.

[49] J. Troe, V.G. Ushakov, *J. Chem. Phys.* 115 (2001) 2628–3621.
[50] Z. Qin, V. Lissianski, H. Yang, W.C. Gardiner Jr., S.G. Davis, H. Wang, *Proc. Combust. Inst.* 28 (2000) 1663–1669.
[51] M. Frenklach, A. Packard, P. Seiler, Prediction uncertainty from models and data, in: *Proceedings of the American Control Conference*. Anchorage, AK, May, 2002, pp. 4135–4140.

Comments

J. Troe, University of Göttingen, Germany. I see problems with this type of optimization of elementary reaction rate coefficients on the basis of macroscopic reaction systems. The conditions of the macroscopic experiments just do not correspond to those of separate studies of the elementary reactions. In particular, pressure-dependent reactions like $H + O_2 + M$ or $HO + CO + M$ depend strongly on the third bodies M. In macroscopic reaction systems, these M may also be H_2O, reactive atoms, or reactive radicals. For the latter, collision efficiencies may differ markedly from the values derived for third bodies like N_2. The optimization of this paper may mix this all up. I would recommend leaving the results, from separate elementary reaction rate studies untouched and only optimize those collision efficiencies (or rate coefficients) that are otherwise inaccessible or unknown.

Reply. We agree that optimization of reaction rate coefficients on the basis of macroscopic reaction systems cannot provide rate values more accurate than isolated "microscopic" experiments or "ab initio" theoretical studies. The purpose of optimization is to examine the ability of up-to-date rate coefficients for predicting the responses of macroscopic reaction systems. This is, after all, the practical purpose of fundamental reaction kinetics. In our optimization procedure, we ask two basic questions. First, do the latest developments in reaction kinetics, i.e., better and more accurate rate coefficients, predict or give rise to better predictions for the macroscopic reaction systems? Second, given the uncertainty in each and every rate parameter, can the responses of macroscopic reaction systems be better predicted by systematic optimization within the uncertainty bounds of each rate parameter? We maintain that the ultimate goal of kinetics studies can only be achieved by fundamental theoretical and experimental studies supplemented frequently by studies such as the one reported here.

The collision efficiencies of different species are indeed markedly different, and it is precisely this reason why we chose to optimize the key, individual collision efficiencies for key pressure-dependent reactions. Uncertainty bounds intrinsically limit to which extent each efficiency factor can be varied, thus maintaining their physical nature, for example, H_2O is a more efficient third body. For this reason, we do not see any fundamental reason why optimization would mix this up. As a practical measure we note that for $H + O_2 + M = HO_2 + M$ the un-optimized third body efficiencies are 0.53, 0.53, 0.75, 12, and 1 for Ar, He, O_2, H_2O, and H_2, respectively, relative to that of N_2, and the optimized efficiency factors are 0.4, 0.46, 0.85, 11.9, and 0.75. These optimized factors are well within their respective range of uncertainties.

•

Juan Li, Princeton University, USA. The rate constant of $CO + OH \Longleftrightarrow CO_2 + H$ is pressure-dependent. The authors provide a new expression of the rate constant by fitting the literature experimental results. However, most of the experimental results were measured at low pressures. Is it proper to use the rate constant expression for high-pressure cases?

Reply. A recent theoretical study [1] showed that the rate coefficient for $CO + OH = CO_2 + H$ starts to deviate from the low pressure limit (by more than 2%) when pressure becomes greater than ca. 20, 80, 700, 3600 and 13000 bar for $T = 800$, 1000, 1500, 2000, and 2500 K, respectively. This suggests that the reaction would indeed be at or nearly at its low-pressure limit under the conditions of all experimental data considered herein. Furthermore, the optimized rate expression agrees to within 5% of the theoretical result of [1] in the temperature range of 800–2500 K.

Reference

[1] A. Joshi, H. Wang, *Int. J. Chem. Kinet*. (2004) submitted for publication.

•

S.S. Kumaran, Cabot Corporation, USA. How does the bath gas βc impart the flame speed map (uncertainties)? What is the relative βc of various bath gases towards other reactions (title reaction) $CO + OH \rightarrow CO_2 + H$?

Reply. The influence of third body efficiencies of certain pressure-dependent reactions on flame speed has been known for quite a while (Ref. [43] in paper). Active efficiency factors were considered in model optimization.

Based on recent theoretical studies, e.g. [1], the $CO + OH$ reaction would indeed be very close to its low-pressure limit under conditions of all experiments considered herein. For this chemical activation process, the impact of various bath gases would therefore be virtually unimportant for the present study.

Reference

[1] A. Joshi, H. Wang, *Int. J. Chem. Kinet*. (2004) submitted.

•

David Smith, University of Leeds, UK. For part of their optimization, the authors use the burning velocity data of McLean (Ref. [32] in paper). The experiments, particularly those with 25% CO/5% H_2 fuel were carefully chosen to have high sensitivity to the CO + OH reaction. Two comments on these data:

1. All expanding spherical flame methods for burning velocity measurements have hot burnt gas inside the flame; thereby prone to radiative heat loss. For these flames (relatively show burning and high CO_2 content), measured burning velocities may be low by up to 4–5%.
2. As reported in the paper, the authors found that computed burning velocities were sensitive to CO + OH rate only at temperatures around 1160 K. Comparison with these experimental data says essentially nothing about CO + OH at other temperatures.

Reply. Radiative heat loss would have little influence on measured flame speeds, as long as you are not near the flammability limits [1,2]. The 95% CO + 5% H_2 in air flame data measured by the expanding spherical flame methods and used as model optimization and validation targets were far from the flammability limits and thus they should be affected minimally by radiative heat loss.

The fact that the CO + OH reaction is influential in a fairly narrow temperature range for the 95% CO + 5% H_2 flames is a very important result. Although comparison with these flame speed data says very little about CO + OH at other temperature, it does point out the subtle fact that a single modified Arrehnius expression cannot reconcile available flame speed and shock tube data of CO. Specifically, a proper prediction for the 95% CO + 5% H_2 flames requires a smaller rate coefficient at temperatures around 1160 K, yet a single modified Arrehnius expression would not be able to reconcile flame speed and shock tube data that are sensitive to the rate coefficient of the CO + OH reaction at higher temperatures.

References

[1] C.K. Law, F.N. Egolfopoulos, *Proc. Combust. Inst.* 24 (1992) 137–144.
[2] G. Rozenchan, D.L. Zhu, C.K. Law, S.D. Tse, *Proc. Combust. Inst.* 29 (2002) 1461–1469.

•

Frederick L. Dryer, Princeton University, USA. Your method of optimization appears to involve adjustments only in the pre-exponent in rate correlations, which results in rate changes at all temperatures. We have shown [1] that there are "temperature windows" for each input parameter (rate constant, diffusion coefficient) where laminar flame speed is most sensitive to the specific parameter. These windows are small in comparison to the total temperature range of the particular flame. Thus in optimizing against all of the different types of experimental targets that were utilized, your method simultaneously adjusts each rate constant at all temperatures while optimizing against a particular target that covers a particular temperature range. Would it not be more appropriate to optimize both the pre-exponent and temperature dependence (functional shape) of each rate correlation? Essentially you forced such a result here for one rate by proposing a different correlation of CO + OH than appears in the published literature. We have shown the importance of adjusting both pre-exponent and temperature dependence of rate correlations for several elementary reactions involved in the H_2/CO/O_2 oxidation mechanism, including this one [2].

References

[1] Work in Progress Poster 1F2-13, *Int. J. Chem. Kin.* (2004) submitted.
[2] Work in Progress Poster 1F1-04, *Int. J. Chem. Kin.* (2004) submitted.

Reply. We agree with the fact that each target (flame speed, ignition delay, and flow reactor) is sensitive to a given input parameter (i.e., reaction rate, diffusion coefficient) at a specific temperature or over a given temperature range, depending on the experimental conditions, including pressure. This is precisely the reason why we chose targets that covered an extensive temperature (880–2625 K) and pressure (0.3–33 atm) range in order to ensure accurate optimization of the input parameter over an extended temperature and pressure range. While we agree that a simultaneous optimization of the pre-exponential and temperature dependence would be more rigorous, this level of optimization was not needed as can be seen by the excellent agreement between model predictions of the optimized model and experimental data over extensive temperature and pressure ranges.

A theoretical analysis by Troe [1] has shown that due to the complexity of the CO + OH reaction, there is no inherent reason to believe that a single modified Arrehnius expression can adequately describe the rate of this reaction over an extended temperature range. We proposed to refit the experimental data for the CO + OH reaction using a summation of two modified Arrehnius expressions to more accurately reconcile the experimental data for high, intermediate and low temperatures. This expression also agrees very well will our recent theoretical result [2].

References

[1] J. Troe, *Proc. Combust. Inst.* 27 (1998) 167–175.
[2] A. Joshi, H. Wang, *Int. J. Chem. Kinet*. (2004) submitted.